Surface Electron Accumulation and the Charge Neutrality Level in In_2O_3

P. D. C. King,[1] T. D. Veal,[1] D. J. Payne,[2] A. Bourlange,[2] R. G. Egdell,[2] and C. F. McConville[1,*]

[1]*Department of Physics, University of Warwick, Coventry CV4 7AL, United Kingdom*

[2]*Chemistry Research Laboratory, Department of Chemistry, University of Oxford, Mansfield Road, Oxford OX1 3TA, United Kingdom*

(Received 6 June 2008; published 11 September 2008)

High-resolution x-ray photoemission spectroscopy, infrared reflectivity and Hall effect measurements, combined with surface space-charge calculations, are used to show that electron accumulation occurs at the surface of undoped single-crystalline In_2O_3. From a combination of measurements performed on undoped and heavily Sn-doped samples, the charge neutrality level is shown to lie ~0.4 eV above the conduction band minimum in In_2O_3, explaining the electron accumulation at the surface of undoped material, the propensity for *n*-type conductivity, and the ease of *n*-type doping in In_2O_3, and hence its use as a transparent conducting oxide material.

DOI: 10.1103/PhysRevLett.101.116808 PACS numbers: 73.20.At, 73.61.−r, 78.66.Li, 79.60.−i

Transparent conducting oxides (TCOs), such as In_2O_3, SnO_2, ZnO and their alloys, represent an important class of materials with applications including transparent electronics, contacts for photovoltaic devices, liquid crystal displays, light emitting diodes and chemical sensors [1–4]. Recently, there has been increased interest in considering single-crystalline thin-film and nanostructured TCO materials as semiconductors in their own right, with potential applications in electronic, short wavelength photonic, and chemical and biological sensor devices [5–9]. In_2O_3, one of the archetypal TCO materials, has received much attention, and indeed implementation [3]; however, even basic material quantities such as its fundamental band gap have proved controversial. A weak onset of optical absorption at around 2.6 eV was originally attributed to an indirect transition, with the direct band gap assigned at 3.75 eV from the onset of significant absorption intensity [10]. However, it has recently been shown [11,12] that the weak onset of absorption is due to dipole forbidden transitions or transitions with only minimal dipole intensity between the topmost valence bands and the conduction band minimum (CBM), rather than the indirect band gap hypothesis. Thus, the direct band gap of In_2O_3 can be identified as only ~2.6 eV [11,13].

In order to fully realize the range of potential device applications, in particular, for its use as contacts, sensors and in nanoscale material where the surface to bulk ratio is much higher than in conventional films, it is crucial to understand the surface electronic properties of the material. In_2O_3 has been reported to exhibit a pronounced depletion of electrons at the surface [14,15]. However, following the revision of the fundamental band gap [11,13] and improvements in growth resulting in high-quality single-crystalline In_2O_3 films [13], these surface space-charge regions need to be reinvestigated. This letter reports an investigation of the surface electronic properties of epitaxial undoped and Sn-doped In_2O_3 using a combination of high-resolution x-ray photoemission spectroscopy (XPS), Hall effect and infrared (IR) reflectivity measurements, combined with space-charge layer calculations. In contrast to previous results, electron accumulation is identified at the surface of undoped In_2O_3 films, and these results are discussed within the context of the charge neutrality level and the bulk bandstructure of the material.

Undoped and Sn-doped In_2O_3(100) films were grown in the bixbyite cubic structure by oxygen plasma-assisted molecular beam epitaxy on yttria stabilized cubic-zirconia (YSZ) (100) substrates at a growth temperature of 650 °C. The In_2O_3 layer thicknesses were 120 nm determined from growth rate calculations, which were themselves calibrated from cross-sectional transmission electron microscopy (TEM) measurements of films grown under identical conditions. No evidence of secondary phases was observed from TEM measurements. Further details of the growth are reported elsewhere [13].

High-resolution XPS measurements were performed using a Scienta ESCA300 spectrometer with a monochromated rotating anode Al-$K\alpha$ x-ray source ($h\nu =$ 1486.6 eV). The effective instrument resolution is ~350 meV. The binding energy is given with respect to the Fermi level calibrated from the Fermi edge of conduction band emission observed in these samples. The position of the valence band maximum (VBM) is determined by extrapolating a linear fit to the leading edge of the valence band photoemission to the background level in order to account for energy broadening [16]. Single-field Hall effect measurements were performed in the van de Pauw geometry at room temperature. IR reflectivity measurements were performed using a Perkin-Elmer Spectrum GX Fourier Transform Infrared Spectrometer, with a 35° specular reflection to the surface normal. A high-reflectivity optical mirror was used as a reference.

Valence band photoemission spectra of undoped and Sn-doped In_2O_3 are shown in Fig. 1. The VBM to surface Fermi level separation is determined from these to be 2.94 and 3.06 eV for the undoped and Sn-doped samples,

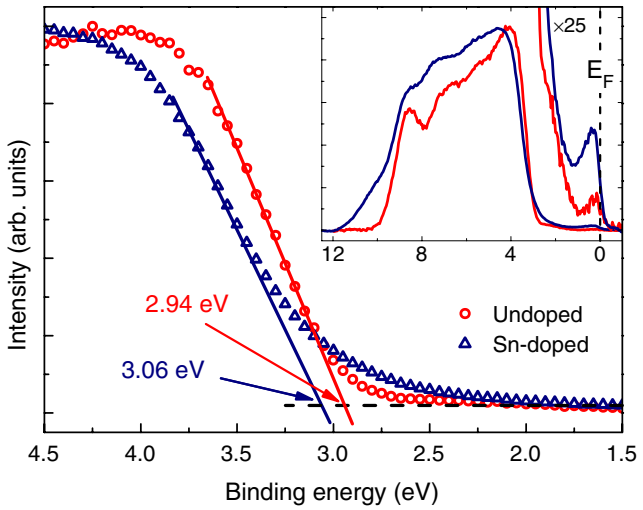

FIG. 1 (color online). Leading edge of the valence band photoemission of undoped and Sn-doped In_2O_3, and the linear extrapolations used to determine the VBM to surface Fermi level separation. The Shirley-background subtracted valence band photoemission spectra are shown over an extended binding energy range inset, with the conduction band emission also magnified ×25.

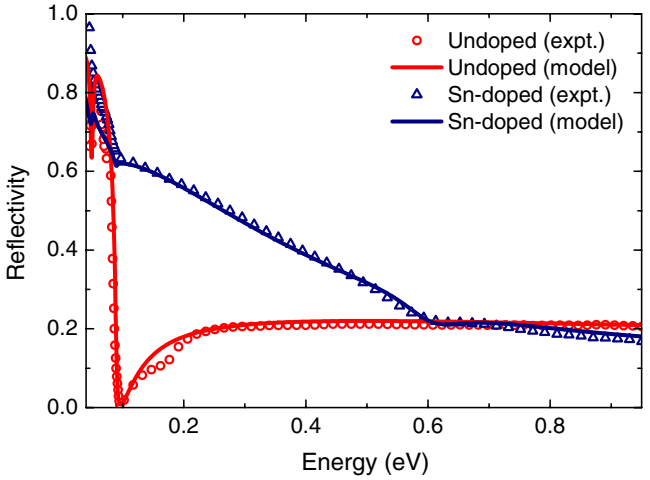

FIG. 2 (color online). IR reflectivity spectra and dielectric theory simulations of undoped and Sn-doped In_2O_3.

respectively, as indicated in the figure. For a direct band gap of 2.62 eV [10], this results in the surface Fermi level being pinned 0.32 and 0.44 eV above the CBM at the surface for the undoped and Sn-doped samples, respectively, consistent with the conduction band emission observed in the photoemission spectra close to the Fermi level, shown inset in Fig. 1.

To understand the surface electronic properties in detail, it is crucial to characterize those of the bulk. Hall effect measurements revealed an electron density and mobility of 7.5×10^{18} cm^{-3} and 32 cm^2 V^{-1} s^{-1} respectively for the undoped In_2O_3 and 4.2×10^{20} cm^{-3} and 27 cm^2 V^{-1} s^{-1} respectively for the Sn-doped In_2O_3. The Kane [17] $\mathbf{k} \cdot \mathbf{p}$ approximation has been used here to describe a nonparabolic conduction band (as is the case for In_2O_3 [12]) within carrier statistics calculations, assuming a band edge electron effective mass of $0.35m_0$ [2], giving bulk Fermi levels 0.02 eV and 0.54 eV above the CBM for the undoped and Sn-doped samples, respectively.

IR reflectivity spectra were also measured, shown in Fig. 2. The extended tail on the reflectivity from the Sn-doped sample is attributed to a heavily damped conduction electron plasma oscillation, indicating a much higher plasma frequency in the Sn-doped than the undoped sample. The lack of observable Fabry-Pérot interference fringes within the measured spectral range is consistent with the 120 nm sample thickness. The reflectivity spectra were simulated using a two-oscillator dielectric theory model to account for lattice and free-carrier contributions. A transfer-matrix method was used to model transmission through the In_2O_3 epilayer and reflections at the air/In_2O_3 and In_2O_3/YSZ (substrate) interfaces, as well as incoherent reflections in the YSZ substrate. The dielectric theory simulations showed good agreement with the experimental data (see Fig. 2), and from these the plasma frequency was determined to be 85 and 600 meV for the undoped and Sn-doped samples, respectively, corresponding to an electron density of 7.4×10^{18} and 4.0×10^{20} cm^{-3}, respectively, in good agreement with the Hall effect results.

Consequently, the VBM to Fermi-level separation is larger at the surface than in the bulk of the undoped In_2O_3, indicating a downward bending of the conduction and valence bands at the surface, relative to the Fermi level, leading to an increase in electron density in the near-surface region. The band bending and carrier concentration profiles as a function of depth below the surface have been calculated by solving Poisson's equation within a modified Thomas-Fermi approximation (MTFA), subject to the boundary conditions of the surface and bulk Fermi level position relative to the VBM, incorporating a nonparabolic conduction band, as described elsewhere [18]. These are shown in Figs. 3(a) and 3(b), revealing a pronounced accumulation of electrons close to the surface, although the carrier concentration still tends to zero right at the surface, as the wave functions must decay to zero amplitude here due to the potential barrier that the surface imposes. The surface electron accumulation observed here is in contrast to the depletion of electrons reported previously at In_2O_3 surfaces [14,15]. The recent revision of the band gap is an important factor in allowing the identification of the electron accumulation; however, fundamentally, it is the comparatively low electron density in the bulk of the undoped sample, resulting from the high growth quality, which means that the bulk Fermi level is sufficiently low to allow the intrinsic electron accumulation to be observed here in In_2O_3. Without detailed information on the bulk Fermi level positions in the samples investigated in Refs. [14,15], it is not possible to comment further on

whether any of those specific samples had low enough carrier densities to exhibit indium oxide's intrinsic electron accumulation.

Electronic surface states in semiconductors, resulting from a breaking of the translational symmetry of the bulk, are either donorlike or acceptorlike where the surface state wave functions have predominantly valence band or conduction band character, respectively [19]. Such surface states can either be neutral (occupied donorlike or unoccupied acceptorlike states), positively charged (unoccupied donorlike states) or negatively charged (occupied acceptorlike states). In the presence of charged surface states, the carriers in the near-surface region of the semiconductor rearrange in order to screen the surface charge, causing an upward or downward bending of the conduction and valence bands with respect to the Fermi level and a space charge that balances the surface charge. The surface electron accumulation observed here for undoped In_2O_3 therefore results from a screening of the positive charge of unoccupied donorlike surface states. Indeed, the Poisson-MTFA calculations reveal a large positive surface state density of $N_{ss} = 7.2 \times 10^{12}$ cm^{-2} associated with the electron accumulation.

The demarcation between surface states that are predominantly donorlike (below) and acceptorlike (above) can be identified as the charge neutrality level (CNL), or branch point energy, of the semiconductor [19]. The existence of unoccupied donorlike surface states in this case means that the Fermi level is pinned slightly below the CNL at the surface. Consequently, the CNL must be located very high relative to the band extrema in In_2O_3, >0.32 eV above the CBM, in contrast to the majority of other semiconductors where it is located within the fundamental band gap. This high relative location can be understood by considering the bulk bandstructure of In_2O_3, which exhibits a particularly low Γ-point CBM compared to the average conduction band edge across the Brillouin zone and a shallow dispersion of the valence bands (see, for example, Fig. 3 in Ref. [12]). Being localized at the surface, electronic surface states have a rather extended $\mathbf{k}$-space nature, and consequently derive their character from the band edges across the entire Brillouin zone. The CNL is therefore located close to the midgap energy averaged across the Brillouin zone [19], and may therefore be expected to lie above the CBM in In_2O_3.

To explore this further, Sn-doped In_2O_3 was investigated, in order to move the bulk Fermi level above the CNL. In this case, the surface Fermi level must pin slightly above the CNL resulting in a negative surface charge from occupied acceptor surface states. Charge neutrality is then maintained by an upward bending of the bands relative to the Fermi level, causing a depletion of electrons at the surface. As the VBM to Fermi level separation is larger in the bulk than at the surface (determined from the Hall effect, IR reflectivity and XPS measurements discussed above), such an electron depletion layer does exist at the surface for heavily Sn-doped In_2O_3, as indicated by the calculated band bending and carrier concentration profiles shown in Fig. 3(c) and 3(d). The pinning of the surface Fermi level slightly below (above) the CNL for the undoped (Sn-doped) In_2O_3 therefore allows experimental limits to be given for the location of the CNL: $2.94 < E_{CNL} < 3.06$ eV above the VBM. Consequently, the CNL lies $\sim$0.4 eV above the CBM in In_2O_3.

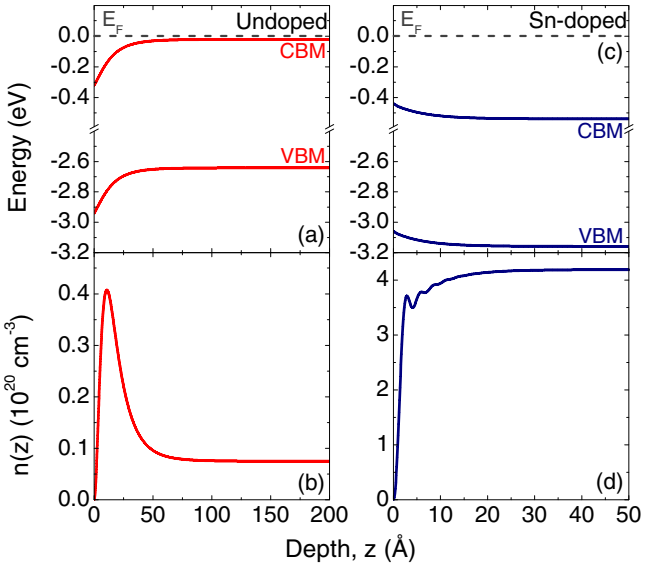

FIG. 3 (color online). (a) [(c)] Band bending and (b) [(d)] carrier concentration profiles in the near-surface region of undoped [Sn-doped] In_2O_3.

As discussed above, the CNL lying so high relative to the band edges is unusual amongst conventional semiconductors. Consequently, surface electron accumulation is also unusual, and has in fact only previously been reported as an intrinsic property of the surface for InAs [20] and InN [21]. The band extrema relative to the CNL estimated here for In_2O_3 and also for these common-cation semiconduc-

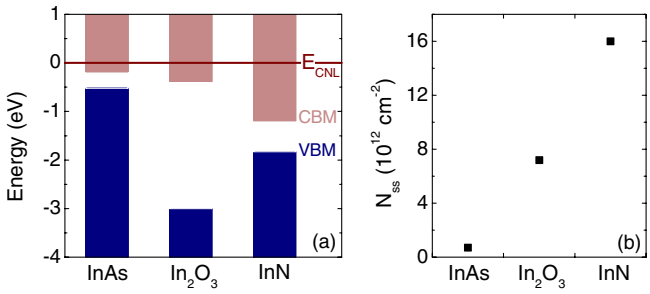

FIG. 4 (color online). (a) Conduction and valence bands of InAs, In_2O_3, and InN relative to the CNL (InAs from Ref. [25]; In_2O_3 determined here; InN from Ref. [22]), and (b) typical sheet density of unoccupied donor surface states associated with electron accumulation in InAs (from Ref. [20]), In_2O_3 (determined here) and InN (from Ref. [26]).

tors are shown in Fig. 4(a). In In_2O_3, the CBM lies further below the CNL than in InAs, but not as far below as in InN, resulting in an areal density of unoccupied donor surface states associated with the electron accumulation between those typical for InAs and InN, as shown in Fig. 4(b). An important factor explaining the CBM lying below the CNL in all of these In-containing compounds is the relatively low energy of the In 5 s orbital. This, coupled with the small *s*-*s* repulsion between the cation and anion *s* orbitals due to the large cation-anion bond length and *s*-orbital energy separation, particularly with N and O, results in a low-lying cation *s*-like CBM compared to the average band edge across the Brillouin zone, resulting in the CBM lying below the CNL [22]. Similar considerations may also apply to other materials with a large size and electronegativity mismatch between the constituent cation and anion, for example, II-O semiconductors such as CdO and ZnO. Consequently, surface electron accumulation may also be expected in these materials.

The position of the CNL relative to the band extrema also has implications for the bulk electronic properties of In_2O_3. Within the amphoteric defect model [23], native defects tend to drive the Fermi level in the bulk towards the CNL. As the CNL lies well above the CBM in In_2O_3, native defects favorably form as donors, increasing the Fermi level, while compensating acceptor defects will have higher formation energies. This, therefore, provides an overriding band-structure explanation of the propensity for In_2O_3 to have a high background electron density even when nominally undoped. The range of Fermi level positions attainable by extrinsic doping has also been shown to be intimately related to the CNL [24], due to an increasing tendency for native defects to form compensating centers as the Fermi level moves away from the CNL. In In_2O_3, the *n*-type doping limit, with the Fermi level some way above the CNL, will therefore lie well above the CBM, meaning that it is possible to achieve extremely high *n*-type conductivities in this material by extrinsic doping (for example, $n \sim 10^{21}$ cm^{-3} for In_2O_3:Sn [3]). Thus, the CBM being located below the CNL in In_2O_3, combined with its relatively large fundamental band gap and dipole forbidden (minimal intensity) optical transitions between the CBM and VBM (high-lying valence bands) [11], explains the ability to obtain In_2O_3 with the usually contradictory properties of transparency and high conductivity, and hence its use as a TCO material.

In conclusion, using a combination of high-resolution x-ray photoemission spectroscopy, IR reflectivity and Hall effect measurements, combined with semiconductor space-charge calculations, single-crystalline undoped In_2O_3 has been shown to exhibit electron accumulation at its surface, in contrast to the majority of other semiconductors. This was explained in terms of the low Γ-point conduction band minimum in In_2O_3 lying below the charge neutrality level. Increasing the bulk Fermi level to above the charge neutrality level by Sn-doping resulted in a depletion of electrons at the surface, allowing the charge neutrality level to be located approximately 0.4 eV above the conduction band minimum. This explains not only the surface electron accumulation, but also both the propensity for *n*-type conductivity in undoped material and the ease of extrinsic *n*-type doping, providing an understanding of the normally conflicting properties of transparency and conductivity in In_2O_3.

We are grateful to D. Law and G. Beamson for technical assistance. This work was supported by the EPSRC, UK, under Grants No. EP/C535553/1 (Warwick), No. GR/S94148 (Oxford), and No. EP/E025722/1 (XPS facility).

*C.F.McConville@warwick.ac.uk

[1] G. Thomas, Nature (London) **389**, 907 (1997).
[2] I. Hamberg and C. G. Granqvist, J. Appl. Phys. **60**, R123 (1986).
[3] C. G. Granqvist and A. Hultåker, Thin Solid Films **411**, 1 (2002).
[4] N. G. Patel, P. D. Patel, and V. S. Vaishnav, Sens. Actuators B Chem. **96**, 180 (2003).
[5] K. Nomura *et al.*, Science **300**, 1269 (2003).
[6] A. Tsukazaki *et al.*, Nature Mater. **4**, 42 (2005).
[7] Z. W. Pan, Z. R. Dai, and Z. L. Wang, Science **291**, 1947 (2001).
[8] Y. Li, Y. Bando, and D. Golberg, Adv. Mater. **15**, 581 (2003).
[9] D. Zhang *et al.*, Nano Lett. **4**, 1919 (2004).
[10] R. L. Weiher and R. P. Ley, J. Appl. Phys. **37**, 299 (1966).
[11] A. Walsh *et al.*, Phys. Rev. Lett. **100**, 167402 (2008).
[12] F. Fuchs and F. Bechstedt, Phys. Rev. B **77**, 155107 (2008).
[13] A. Bourlange *et al.*, Appl. Phys. Lett. **92**, 092117 (2008).
[14] A. Klein, Appl. Phys. Lett. **77**, 2009 (2000).
[15] Y. Gassenbauer *et al.*, Phys. Rev. B **73**, 245312 (2006), and references therein.
[16] S. A. Chambers, T. Droubay, T. C. Kaspar, and M. Gutowski, J. Vac. Sci. Technol. B **22**, 2205 (2004).
[17] E. O. Kane, J. Phys. Chem. Solids **1**, 249 (1957).
[18] P. D. C. King, T. D. Veal, and C. F. McConville, Phys. Rev. B **77**, 125305 (2008).
[19] W. Mönch, *Semiconductor Surfaces and Interfaces* (Springer, Berlin, 2001).
[20] M. Noguchi, K. Hirakawa, and T. Ikoma, Phys. Rev. Lett. **66**, 2243 (1991).
[21] I. Mahboob *et al.*, Phys. Rev. Lett. **92**, 036804 (2004).
[22] P. D. C. King *et al.*, Phys. Rev. B **77**, 045316 (2008).
[23] W. Walukiewicz, J. Vac. Sci. Technol. B **5**, 1062 (1987).
[24] W. Walukiewicz, Physica (Amsterdam) **302–303B**, 123 (2001).
[25] V. N. Brudnyi, S. N. Grinyaev, and N. G. Kolin, Semiconductors **37**, 537 (2003).
[26] P. D. C. King *et al.*, Appl. Phys. Lett. **91**, 092101 (2007).